Predicting Porosity through Simulating Sandstone Compaction and Quartz Cementation[1]

R. H. Lander[2] and O. Walderhaug[3]

ABSTRACT

Presently available techniques for predicting quantitative reservoir quality typically are limited in applicability to specific geographic areas or lithostratigraphic units, or require input data that are poorly constrained or difficult to obtain. We have developed a forward numerical model (Exemplar) of compaction and quartz cementation to provide a general method suited for porosity prediction of quartzose and ductile grain-rich sandstones in mature and frontier basins. The model provides accurate predictions for many quartz-rich sandstones using generally available geologic data as input. Model predictions can be directly compared to routinely available data, and can be used in risk analysis through incorporating parameter optimization and Monte Carlo techniques.

The diagenetic history is modeled from the time of deposition to present. Compaction is modeled by an exponential decrease in intergranular volume as a function of effective stress. The model is consistent with compaction arising from grain rearrangement, ductile grain deformation, and brittle failure of grains, and accounts for the effects of fluid overpressures and stable grain packing configurations. Quartz cementation is modeled as a precipitation-rate–controlled process according to the method of Walderhaug (1994, 1996) and Walderhaug et al. (in press).

Input data required for a simulation include effective stress and temperature histories, together with the composition and texture of the modeled sandstone upon deposition. Burial history data can be obtained from basin models, whereas sandstone composition and texture are derived from point-count analysis of analog thin sections. Exemplar predictions are consistent with measured porosity, intergranular volume, and quartz cement fractions for modeled examples from the Quaternary and Tertiary of the Gulf of Mexico Basin, the Jurassic of the Norwegian shelf, the Ordovician of the Illinois basin, and the Cambrian of the Baltic region.

INTRODUCTION

Reservoir quality is one of the important uncertainties in wildcat drilling (Bloch, 1994a; Wilson, 1994). Present approaches to reservoir quality prediction, however, commonly are limited in applicability, are difficult to apply, or are of unproven accuracy. The need for improved methods has motivated us to develop a model, known as Exemplar, that is designed to

- Consider the most significant porosity controlling processes in sandstone lithologies that are common hydrocarbon reservoirs
- Make predictions that approach the measurement accuracy of available data
- Use input data that are commonly available, easily obtained, or readily estimated in both mature and frontier basin settings
- Produce predictions that can be compared directly to petrographic thin sections
- Include a rigorous approach to uncertainty assessment so that reservoir quality predictions can be stated in probabilistic terms
- Be fast and easy to use on personal computers available to explorationists

In our initial efforts we have targeted quartz-rich sandstones because they are the most common sandstone reservoir type and because their porosity commonly is controlled by just two classes of diagenetic processes: compaction and quartz cementation. In this paper, we review the model's design and algorithms, give conceptual justifications for the approaches we have used, and present some

[1]Manuscript received August 14, 1997; revised manuscript received June 19, 1998; final acceptance October 5, 1998.

[2]Geologica, P.O. Box 8034, N-4003 Stavanger, Norway; e-mail: rhl@geologica.no

[3]Statoil, 4035 Stavanger, Norway; e-mail: OWALD@statoil.no

We thank Esso Norge a.s and Exxon Production Research Company for providing the funding to implement and test Exemplar, and Stan Paxton, David Awwiller, et al., from Exxon Production Research for their valuable guidance in this work. Finally, we thank Linda Bonnell, Sal Bloch, Alton Brown, and Dick Larese for their thorough reviews of earlier versions of this manuscript.

Table 1. Exemplar Output Results for Each Model Time Step

Rock Fractions	Porosity Quartz cement Nonquartz cement Intergranular volume Quartz grains Nonquartz framework grains Matrix
Rock Volumes (cm^3)	Bulk rock volume Quartz cement (for current time step) Quartz cement (cumulative) Nonquartz cement (cumulative)
Rates (cm^3/m.y.)	Quartz cementation Nonquartz cementation Compaction
Porosity Controls	Copl—absolute porosity loss due to compaction (Ehrenberg, 1989) Cepl—absolute porosity loss due to cementation (Ehrenberg, 1989) ICOMPACT: copl / (copl + cepl) (Lundegard, 1991)
Other	Quartz surface area (cm^2) Average overgrowth thickness (mm) $\%R_o$ (Sweeney and Burnham, 1990)

example simulations. The model provides reasonably accurate reservoir quality predictions for quartzarenites, sublitharenites, and subarkoses, and has proven to be a useful predictive tool for both mature and frontier regions. The model also appears to be well suited to porosity prediction of ductile grain-rich rocks, but more geologic data sets are needed for calibration before it can be confidently applied to reservoir quality prediction in such lithologies.

Exemplar simulates the evolution of sandstone porosity and composition throughout the geologic history of the modeled unit. In addition, it simulates the rates of porosity reduction due to compaction and cementation through time (output data types are given in Table 1). Input data needed to conduct a simulation include a description of the texture and composition of the sandstone upon deposition, burial history information, and parameter values for the compaction and quartz cementation algorithms. Depositional sandstone texture and compositional data are derived from standard petrographic analyses of reservoir samples from nearby wells or from lithologic analogs in frontier areas. Basin modeling results for prospect reservoir intervals provide the necessary temperature and effective stress history input (burial depth can be substituted for effective stress for areas that have not experienced significant fluid overpressures). Finally, the appropriate compaction and quartz cementation parameters can be obtained from calibration studies. A listing of input data types that can be used by the model is given in Table 2.

In addition to its utility for porosity prediction prior to drilling, Exemplar has proven to be a useful paleothermal indicator (Awwiller and Summa, 1997; Lander et al., 1997a, b). Because quartz cementation is strongly controlled by burial history, the model can be used to constrain burial histories by comparing model predictions with measured values. Exemplar also may provide a more accurate depiction of reservoir quality variations and heterogeneties within fields than do pure geostatistical methods when it is used in concert with upscaling techniques; furthermore, the model should provide a more accurate basis for assessing the evolution in properties of sandstones that act as hydrocarbon carrier systems than do current basin modeling systems.

EXISTING APPROACHES TO RESERVOIR QUALITY PREDICTION AND COMPARISON WITH EXEMPLAR CONCEPTUAL FRAMEWORK

Existing reservoir quality models tend to fall into two categories (Wood and Byrnes, 1994): effect-oriented models, such as statistical correlations of porosity with other variables, and process-oriented models, such as geochemical reaction-path models that are based on the thermodynamics and kinetics of minerals, aqueous species, and gases. The statistical

Table 2. Input Parameters for Exemplar Simulations

Initial Sediment Composition	Porosity (%)
	Quartz framework grain (%)
	Nonquartz framework grain (%)
	Matrix (%)
	Average grain diameter (mm)
Compaction Parameters	IGV_f—stable packing intergranular volume (%)
	β—exponential rate of intergranular volume loss with effective stress (1/MPa)
	Quartz cement abundance sufficient to arrest compaction (%)
Quartz Cementation Parameters	Quartz precipitation rate preexponential constant (mol/cm^{2}s)
	Quartz precipitation rate exponential constant (1/°C)
	Minimum temperature necessary for the onset of quartz precipitation (°C)
Burial History	Temperature (°C), time (m.y.)
	Burial depth (m), time (m.y.)
	Effective stress (MPa), time (m.y.) (or use burial depth and assume hydrostatic pressure)
	Grain coat completeness (%), time (m.y.)
	Nonquartz cements (cm^3), time (m.y.)

approach can be accurately applied to sandstones with less than 10% cement, but this approach breaks down for more highly cemented sandstones (Bloch, 1991). An additional shortcoming to the statistical approach is that accurate model predictions are constrained to sandstone compositions, textures, and geologic settings represented by the samples included in calibration data sets (Bloch and Helmold, 1994). Thus, it is difficult to apply the empirical approaches to frontier areas with little or no data, to mature areas where statistical studies have yet to be undertaken, or to depth ranges outside that of an existing calibration data set.

Geochemical models, such as those reviewed by Meshri (1990) and Wood (1994), are appealing because by using a first-principle approach to simulating diagenetic reactions they should ideally be more broadly applicable than empirical methods. Although reaction-path models provide important insights into diagenetic processes, in practice the present generation of models is difficult to apply to quantitative porosity prediction. Many such models ignore compaction, frequently the single greatest cause of porosity reduction (Lundegard, 1991), as well as the effect of diagenesis on the surface area of reactive minerals. These models suffer from substantial uncertainties in kinetic and thermodynamic constants because many phases have not yet been characterized, and the extent to which the existing data can be extrapolated from laboratory conditions to geologic time scales and environments is not always clear. Finally, most reaction-path models do not explicitly distinguish between the detrital or authigenic occurrence of minerals, making it difficult to compare predictions with petrographic data.

The approach that we have taken to reservoir quality prediction attempts to synthesize effect-oriented and process-oriented methods. Although the model predicts the result of diagenetic processes, it does not employ a first-principle approach to simulating these processes. Instead, our "hybrid simulator" [terminology of Wood and Byrnes (1994)] employs process algorithms with input parameters that are empirically calibrated to geological data sets. The advantage of using this approach is two-fold. First, by calibrating individual processes, the model should have wider applicability than the standard statistical approach and can be based on data reflecting geologic time durations and environments rather than laboratory conditions. Second, the computational efficiency of a hybrid model can be improved by orders of magnitude compared to a first-principles approach. Greater computational efficiency is important because it permits predictive uncertainties to be evaluated much more rigorously. A thorough investigation of uncertainties is a prerequisite to quantitative, probabilistic approaches to reservoir quality prediction.

A hybrid approach to porosity modeling was also taken by Waples and Kamata (1993) for a variety of lithologic types, including sandstones. Similar to Exemplar, the model used by Waples and Kamata is calibrated against geological data sets and is more widely applicable than the empirical models it was designed to replace. Although this approach succeeds in its goal to improve on the methods used by basin models, it was not designed for reservoir quality prediction (Waples and Kamata, 1993). Consequently, it does not take into consideration the important effects that variations in texture and composition have on porosity. By

contrast, Exemplar uses sandstone textural and compositional data as input. In the present version, the model targets quartz-rich and ductile grain-rich sandstones because the majority of producing sandstone reservoirs are represented by these lithologies, and because the primary controls on porosity can be linked to compaction and quartz cementation. In addition, the model explicitly predicts indices of compaction and cementation that can be directly compared with petrographic analyses of thin sections, making it straightforward to assess the predictive accuracy of the results, as well as to calibrate model parameters.

MODEL DESIGN

Exemplar is designed to predict porosity in sandstones where porosity is dominantly controlled by compaction and quartz cementation. This porosity prediction is directly comparable to petrographically determined intergranular porosity, but not to core analysis porosity, which also may contain secondary porosity, fracture porosity, and microporosity (Pittman, 1979).

Controls on Compaction

Compaction in sandstone is the reduction in bulk rock volume that occurs in response to four classes of processes (in the generally accepted order of importance): grain rearrangement, plastic deformation, dissolution, and brittle deformation (Wilson and Stanton, 1994). In our assessment, a model relating the effects of grain rearrangement, plastic deformation, and brittle deformation to effective stress should provide an adequate basis for simulating compaction in most quartzose and ductile grain-rich sandstones.

We have disregarded grain-to-grain "pressure" dissolution in the present version of the model because we see little empirical evidence of it being a primary control on reservoir quality for the targeted group of sandstone lithologies. Quartzose hydrocarbon reservoirs typically show little evidence for extensive dissolution of quartz except where clay rims occur (Heald, 1956; Thomson, 1959; Wilson, 1984; Houseknecht, 1988) or at stylolites (Sippel, 1968; Land and Dutton, 1978; Suchecki and Bloch, 1988; Ehrenberg, 1990; Paxton et al., 1990; Ajdukiewicz et al., 1991; Bloch, 1991; Szabo and Paxton, 1991; Bjørkum, 1994). Although grain dissolution at stylolites is common, such dissolution has little effect on rock properties of reservoir intervals at the thin-section or core-plug level.

The significance of secondary porosity caused by feldspar and rock fragment dissolution for reservoir quality remains controversial. Giles and de Boer (1990) and Bloch (1991, 1994b, c), in their reviews of the topic, concluded that the significance of secondary porosity commonly is overstated; furthermore, they point out that where secondary porosity does occur it has little effect on the accuracy of porosity predictions because it is counterbalanced by the local reprecipitation of the dissolved material.

Grain rearrangement leads to compaction when framework grains move into tighter packing configurations, and correlates with the stress transmitted through framework grains. A number of petrographers regard grain rearrangement as the primary control on compaction of well-sorted sandstones that are poor in matrix and ductile grains. Exxon workers reported that a stable packing configuration represented by an intergranular volume (IGV) of 26% is reached through grain rearrangement by approximately 2 km burial depth for well-sorted samples (Paxton et al., 1990; Ajdukiewicz et al., 1991; Szabo and Paxton, 1991). Other workers have suggested that such a stable packing configuration cannot be achieved without some minor dissolution at grain contacts sufficient for grains to slip past each other (e.g., Füchtbauer, 1967). Palmer and Barton (1987) contended that rearrangement reduces IGV to a minimum of 34%, and that further compaction requires some grain dissolution. Siever and Stone (1994) asserted that grain rearrangement accounts for an IGV decline to approximately 31%, and that a stable packing configuration of 24% IGV requires minor pressure solution. Although there is some disagreement as to the minimum IGV attained through grain rearrangement alone, most workers agree that the process is a major factor in controlling compaction, and that it can be related to effective stress.

Plastic deformation of grains takes place when grains deform under stress and is the primary control on compaction in ductile grain-rich rocks (Pittman and Larese, 1991). Bulk compaction occurs in response to plastic deformation because it leads to consolidation as pores collapse or are invaded by deforming grains, and because it promotes additional grain rearrangement. The extent of compaction due to ductile grain deformation is a function of the abundance and ductility of ductile grains and the effective stress (Pittman and Larese, 1991). A compaction model based on correlations with effective stress should provide a good basis for simulating the effects of plastic deformation so long as the model can take into account the effect of differing amounts and types of ductile grains.

Brittle grain deformation commonly is thought to play only a minor role in compaction (Wilson and Stanton, 1994). Recent studies employing cathodoluminescence techniques suggest the significance of

brittle grain failure, however, may be underestimated in some settings. Using cathodoluminescence, we have observed numerous healed fractures in quartz grains from Miocene sandstones from the Gulf of Mexico. Similar features in quartzose sandstones have been reported from other regions (Dunn, 1994; S. Bloch, 1994, personal communication; Laubach, 1997). Because brittle grain failure occurs in response to grain-to-grain stress, effective stress should provide a suitable basis for a compaction model incorporating this process.

Simulation of Compaction

A hybrid compaction model should be able to account for the salient points discussed if compaction is modeled as a function of effective stress, and if the effects of grain ductility, sorting, and size are taken into account. A requirement for such a model is that it should provide predictions that can be directly compared to an index of sandstone compaction so that the model can be calibrated and so that uncertainty in model predictions can be quantitatively assessed.

A difficulty in constructing and testing compaction models is that there are no known direct measures of the extent of compaction in sandstones (Wilson and Stanton, 1994). As a result, compaction can be evaluated in sandstones only by using indirect measures and by assuming a depositional porosity based on analogs. Examples of indirect measures of compaction that have been developed include a contact index (Taylor, 1950), a tight packing index (Wilson and McBride, 1988), and an intergranular volume (IGV) (Paxton et al., 1990; Ajdukiewicz et al., 1991; Szabo and Paxton, 1991), which are defined, respectively, as the average number of intergranular contacts per grain; the average number of long, concavo-convex, and sutured contacts per grain; and the sum of intergranular porosity and cements. Although the contact and tight packing indices are useful measures of compaction, McBride et al. (1990) reported that the measures are highly subjective and that they cannot be derived from standard point-count analyses of thin sections. We use IGV as an indirect measure of compaction for the model because it ideally should be less prone to measurement subjectivity, can be determined from standard point-count data, and can be used directly in the simulation of intergranular porosity when cement volumes are also known.

Existing porosity vs. effective stress (or depth) functions provide a good basis for building a compaction model. Empirical functions incorporating burial depth have been used for accurate porosity predictions for sandstones with less than 10% cements so long as they also incorporate sandstone textural and compositional parameters (Bloch, 1991). Porosity decline functions (e.g., Athy, 1930) have been modified for use in basin modeling systems to account for the effects of fluid overpressures by substituting effective stress for burial depth (Ungerer et al., 1990; Schneider et al., 1994). We make two additional modifications to adapt the approach to simulation of the effects of sandstone compaction. IGV, an indirect index of compaction, is substituted for porosity, and we introduce a term representing the stable packing configuration of sandstones. The resulting compaction function is

$$IGV = IGV_f + \left(\phi_0 + m_0 - IGV_f\right)e^{-\beta\sigma_{es}} \qquad (1)$$

where IGV is the sum of pore space, cements, and matrix material (volume fraction); IGV_f is the stable packing configuration (volume fraction); ϕ_0 is the depositional porosity (volume fraction); m_0 is the initial proportion of matrix material (volume fraction); β is the exponential rate of IGV decline with effective stress (MPa^{-1}); and σ_{es} is the maximum effective stress (MPa).

Because matrix material generally has little or no compressive strength, IGV here is defined as including matrix material and intergranular pore space and cement. We also assume that matrix material in grain-supported sandstones does not compact significantly, and that no cements occur at the time of deposition of the sand when the effective stress is zero.

The frame of reference for the model is a 1-cm^3 volume defined by uncompacted sediment at the depositional surface. This reference frame is comparable in scale to thin sections and core plugs, the basic data sources for evaluating and calibrating simulation results. The bulk compaction of the rock can be obtained from the following expression:

$$v = v_0\left(\frac{1-\phi_0' - m_0'}{1-IGV'}\right) \qquad (2)$$

where v is the bulk volume of the compacted rock (cm^3), v_0 is the bulk rock volume upon deposition (cm^3), IGV is the sum of intergranular pore space, cements, and matrix material in the current time step (volume fraction), ϕ_0' is the porosity upon deposition (volume fraction), and m_0' is the matrix material upon deposition (volume fraction).

Although the model conserves the volumes and densities of detrital materials, it does not attempt to maintain mass balance of pore fluids or cements. Through the course of a simulation, the net volume of pore fluid typically is reduced, whereas the net volume of solids increases. The modeled compaction

applies only to the frame of reference and not necessarily to the depositional unit as a whole. When cementation occurs, the overall unit compaction exceeds that of the sample due to dissolution in the source regions for quartz cement (stylolites).

Because sandstones exhibit negligible decompaction with unloading at the model scale of observation, compaction is not reversible in the model even in cases where effective stress decreases, such as after uplift and erosion. Compaction will also terminate when a specified amount of quartz cement has precipitated, strengthening the sandstone framework. The strengthening effect of quartz cementation may be partly responsible for the occurrence of abundant quartz cement in some sandstones with anomalously high IGV values (e.g., >30%). Minor amounts of quartz cement that precipitate prior to achievement of a stable packing configuration could retard compaction until deeper burial provides sufficiently high temperatures for quartz cements to fill remaining pore space. Such a scenario is consistent with compaction experiments of Pittman and Larese (1991), where they evaluated the effect of small amounts of quartz cement on the mechanical strength of ductile grain-rich sandstones. In their experiments, they used a starting material comprised of 22% green shale rock fragments, 40% quartz grains, and 38% porosity. In the absence of quartz cement, the sample compacted to an IGV of 8.8% at an effective stress of 51.7 MPa. An otherwise identical sample with 5.5% quartz cement artificially grown prior to compaction was more resistant to compaction, maintaining an IGV of 19.3% at 51.7 MPa.

Cementation

Quartz Cementation

A number of quartz cementation mechanisms have been proposed for quartzose sandstones, including coupled cementation and compaction arising from pervasive intergranular pressure solution, precipitation of quartz cements from cooling fluids, and diffusion-controlled derivation of quartz cement from nearby shales. Previous models of quartz cementation based on these mechanisms cannot account for the lack of significant intergranular dissolution that occurs in most quartz-cemented sandstones that are free of clay-coated grains, call upon unrealistically extensive fluid fluxes, or predict more pronounced gradients in quartz cement abundance away from cement sources than has been observed in typical reservoir sandstones (Walderhaug, 1996; Walderhaug et al., in press).

By contrast, Exemplar incorporates a model of quartz cementation that assumes that (1) the quartz cement is derived from nearby stylolites or protostylolites (i.e., regions where quartz grains come in contact with clay-rich zones such as clay laminae or silty interbeds), (2) of the three steps that control the quartz cementation process, silica dissolution, diffusion/advection, and precipitation, silica precipitation is the rate-limiting or controlling step, (3) the surface area available for quartz cement precipitation is a function of the size, fraction, and extent of coating of quartz grains, as well as of the overall rock porosity, and (4) no quartz dissolution occurs within the frame of reference for the simulation. The model honors petrographic (cathodoluminescence) evidence showing little evidence of extensive intergranular dissolution (Suchecki and Bloch, 1988). In the following section, we briefly review the important elements of the quartz cementation model and its implementation in Exemplar. For more detail on how the model was derived and how it compares with other models of quartz cementation, see Walderhaug (1994, 1996) and Walderhaug et al. (in press).

The essential elements of the quartz cementation model are the kinetics of quartz precipitation and the surface area available for quartz cement growth. The rate of quartz cementation per unit of surface area has been shown empirically to be a function of temperature (Walderhaug, 1994):

$$r = a10^{(bT)} \tag{3}$$

where a is the quartz precipitation rate preexponential constant (mol/cm^2 s), b is the quartz precipitation rate exponential constant (°C^{-1}), and T is temperature (°C).

This function can be extended to calculate the total amount of quartz cement precipitated during an increment in time by taking into account the surface area available in the sandstone for precipitation of quartz cement, and by considering the temperature range experienced by the sample

$$qcv = \frac{m}{\rho} A a \int_0^t 10^{b(c_n t + d_n)}\, dt \tag{4}$$

where qcv is the volume of quartz that precipitates (cm^3), m is the molar weight of quartz (60.08 g/mol), ρ is the density of quartz (2.65 g/cm^3), A is the quartz surface area (cm^2), t is the duration of the time step (m.y.) converted to seconds, a is the quartz precipitation rate preexponential constant (mol/cm^2 s), b is the quartz precipitation rate exponential constant (1/°C), and c_n and d_n are constants for each time step n (derived from the sample's temperature history).

Quartz surface area plays an important role in controlling the net rate of quartz cementation, as shown in equation 4. Quartz surface area in the model is a function of the abundance of detrital quartz grains in the initial sediment, the average quartz grain size, and the porosity through time:

$$A = (1 - coat)\left[\frac{6\,qgf_0 v_0}{D}\left(\frac{\phi}{\phi_0}\right)\right] \quad (5)$$

where A is the quartz surface area for the present time step (cm^2), qgf_0 is the abundance of quartz grains in initial sediment (fraction), v_0 is the initial rock volume (cm^3), D is the average diameter of initial quartz grains (cm), ϕ is the porosity for the present time step (fraction), ϕ_0 is the initial porosity (fraction), and *coat* is the quartz surface area that is coated and thus unable to act as a substrate for further quartz precipitation (fraction).

The surface area definition assumes that the quartz grains are spherical and are of uniform size. Surface area is modeled to decrease as a function of porosity to account for the effects of compaction and cementation (Figure 1). Compaction reduces quartz surface area by increasing grain contact area, as well as by the injection of matrix material into pore spaces. Cementation can cause surface area reduction when quartz grains are encased by pore-filling cements. The model also assumes that coatings on quartz framework grains reduce surface area proportionally to the coated area. The coat variable in equation 5 refers to the proportion of quartz surface area that no longer permits nucleation of overgrowths because of the occurrence of grain-coating materials. Grain coatings are associated with detrital materials, such as clays and Fe-oxyhydroxides, as well as with authigenic phases, such as clay minerals, carbonate (siderite), or microcrystalline quartz.

Nonquartz Cementation

The model permits the occurrence of cements other than quartz to be defined through time. Although the model does not yet simulate the precipitation of such cements, it does consider the effect that they can have on compaction, quartz precipitation, and porosity. Occurrence of nonquartz cements can reduce the extent of compaction by filling pore space when modeled IGV values exceed the stable packing configuration. In addition, nonquartz cement can reduce the abundance of quartz cement by reducing available pore space and by retarding the net rate of quartz cementation by reducing the available surface area. The model permits the amount of nonquartz cements to vary with time.

Overview of the Simulation Sequence

After the parameter values and model options are defined and the simulation is initiated, the program begins by reading input parameters and by making various initial calculations, such as unit conversions and rock component volume determinations. The model then begins to step forward through time using time-step durations that are selected dynamically based on the rate of change in modeled porosity. Time steps are typically no less than 10^5 yr. The calculations for a given time step are done in the following sequence: compaction, precipitation (or dissolution) of nonquartz cements, quartz surface area, and quartz cement volume. The compaction and cementation calculations are not directly coupled because compaction most likely adjusts more rapidly to changes in burial conditions than cementation, and because compaction commonly dominates the early diagenetic evolution of sandstones. Typical execution times are on the order of seconds for desktop computers for a simulation ranging from the time of burial to the present day.

MODEL CALIBRATION

Compaction

Our compaction model contains three terms that reflect the texture and composition of sandstones: ϕ_0 (depositional porosity), IGV_f (stable packing configuration), and β (exponential rate of compaction with effective stress). Values for the ϕ_0 term can be taken from measurements of near-surface sandstone porosities or artificially mixed and packed sandstones. Although the depositional porosity is largely independent of sandstone composition, it is strongly controlled by texture. Well to moderately sorted fluvial and beach sandstones have depositional porosities of 47.5 ±3.2% (Atkins and McBride, 1992), but more poorly sorted samples have values that are as much as 10–20% lower due to greater packing efficiency of grains (Beard and Weyl, 1973; Clarke, 1979; Dickinson and Ward, 1994).

The IGV_f and β terms are obtained through empirical calibration. We calibrated IGV_f for rigid grain-rich rocks by using 218 well to moderately sorted samples with less than 10% matrix and less than 10% nonquartz cements. The samples are from the Norwegian continental shelf, are of Jurassic and Cretaceous age, and were analyzed by us, as well as by Ehrenberg (1990, 1991, 1993) and S. N. Ehrenberg (1995, personal communication). The samples show present-day IGV values of 28.0 ±5.6% and show no significant variation with estimated maximum effective stress values over a range of from

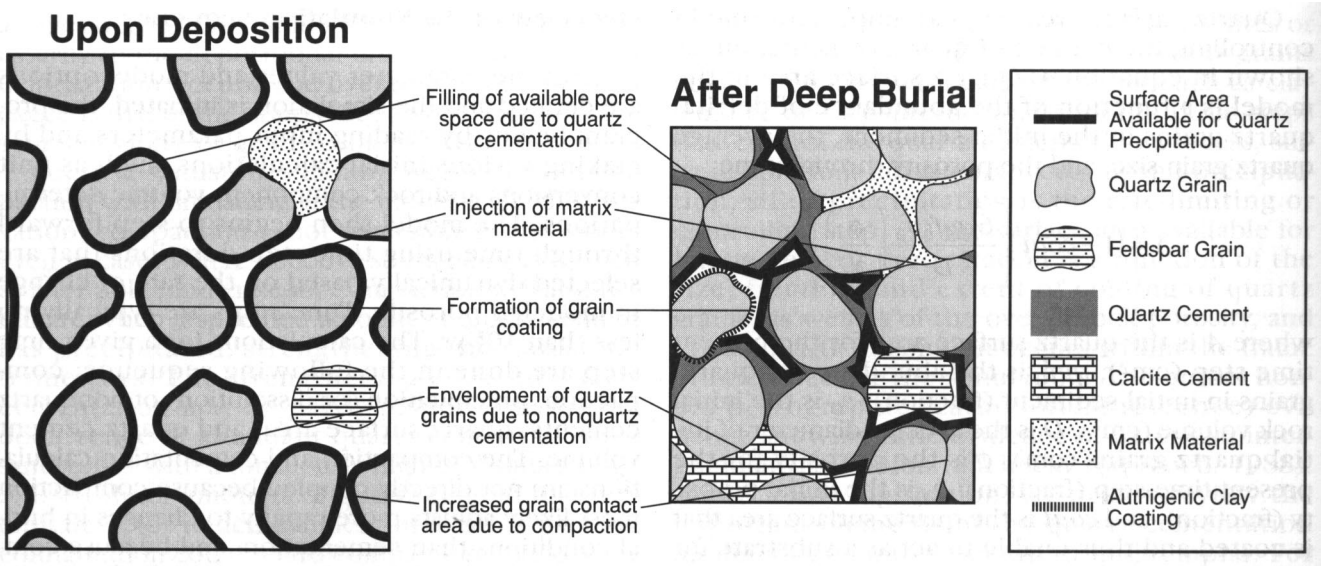

Figure 1—Causes of surface area reduction during sandstone diagenesis.

around 25 to 55 MPa. This lack of variation suggests that the samples are at or near their minimum compacted IGV values. As a result, the values can be used to define the IGV_f term in the compaction function. The values are in good agreement with previously reported values for rigid grain-rich sandstones from other basins (Paxton et al., 1990; Ajdukiewicz et al., 1991; Szabo and Paxton, 1991).

The β term is best constrained using samples that have not achieved stable packing configurations. To calibrate β for rigid grain-rich rocks we used the data of McBride et al. (1990) for Texas Eocene sandstones that have been exposed to maximum effective stresses ranging from about 10 to 50 MPa. A value of 0.06 MPa^{-1} provides a good correspondence between model predictions and measurements (Figure 2).

The most thoroughly documented study of the effects of lithic fragments on compaction has been made by Pittman and Larese (1991). They conducted an extensive set of compaction experiments using quartz grains mixed in various proportions with volcanic, sedimentary, and metamorphic rock fragments. Correspondence between IGV predictions and measurements for the data set are shown as a function of effective stress in Figure 3, and the associated calibrated parameters are listed in Table 3. Over 85% of the model IGV predictions occur within the theoretical 95% confidence interval for point-count analysis. Virtually all of the predictions that are found outside of the confidence interval correspond to experiments conducted at low effective stress values where the experiment results should be expected to diverge most strongly from natural sandstone behavior. In their experiments, Pittman and Larese (1991) used a Vibratool™ to initiate grain rearrangement before compressing the samples, resulting in IGV values of 32.2 ±3.7%. The Exemplar calibrations, however, assume initial porosities of 38% to simulate compaction of natural samples more realistically.

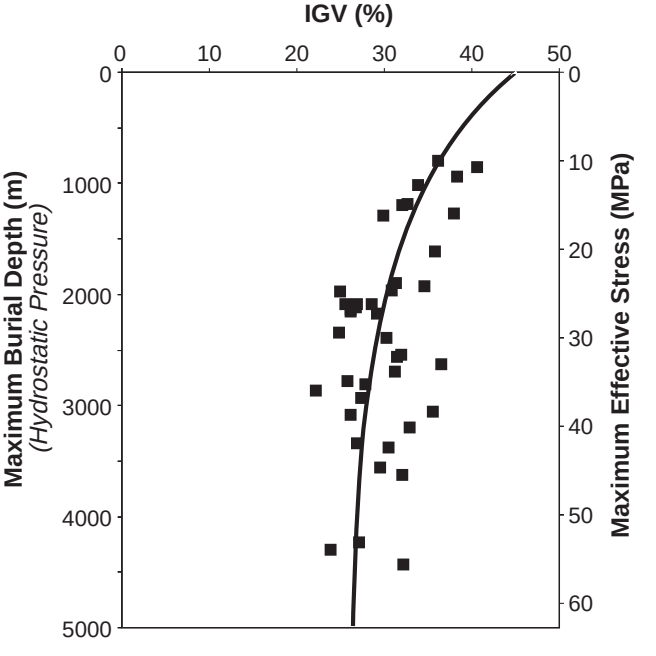

Figure 2—Calibration of the Exemplar compaction model for well sorted to moderately well sorted, rigid grain-rich sandstones. The petrographic data are from McBride et al. (1990). IGV = intergranular volume.

Table 3. Calibrated Compaction Parameters

	Rigid Grains	Weathered Basalt			Shale			Slate		
		25%	50%	75%	25%	50%	75%	25%	50%	75%
IGV_f*	28	22	6	0	22	6	0	24	19	13
β**	0.06	0.06	0.06	0.15	0.06	0.06	0.06	0.06	0.06	0.06

*IGV_f = stable packing intergranular volume (%).
**β = exponential rate of intergranular volume loss with effective stress (1/MPa).

Unfortunately, no other ductile grain-rich data sets were available to test the calibrated compaction functions. Although the experimental compaction trends provide useful insights into the behavior of ductile grain-rich sandstones, the model IGV decline functions for ductile grain-rich sandstones probably should be considered to represent the maximum likely IGV end members. Greater extents of compaction may occur given more realistic burial rates (Kurkjy, 1988) and can be defined in the model by decreasing the IGV_f term.

Note that all compaction data could be matched using a β value of 0.06 MPa^{-1} (with the exception of the highly ductile sandstone comprised of 75% weathered basalt grains). The apparent insensitivity of β to sandstone composition suggests that rates of stress increase are generally of second-order importance in controlling the extent of compaction. By contrast, the IGV_f term is highly variable depending on the mechanical strength of the sandstone. These results indicate that whereas β can be assumed to be a constant for all but the most ductile of sandstones, IGV_f must be empirically calibrated for specific sandstone compositional and textural types.

Quartz Precipitation Kinetics

Using *a* and *b* parameters calibrated to Jurassic sandstones of the Norwegian shelf, we tested quartz cement predictions for two data sets that represent end members in time and temperature histories. Cambrian quartzarenites from the Baltic shield represent a low-heating-rate end member with maximum burial temperatures of approximately 90°C. The second test data set lies at the opposite end of the time and temperature spectrum and is composed of Pliocene–Pleistocene sandstones from the Gulf of Mexico Basin that reached temperatures of as much as 140°C.

Model predictions match measured values within measurement uncertainties (Figure 4), suggesting that the kinetic parameters derived from calibration to the Jurassic sandstones of the Norwegian continental shelf are applicable to sandstones with wide ranges in burial histories.

APPLICATION OF EXEMPLAR TO RESERVOIR QUALITY ANALYSIS

Present-day sandstone porosity is a function of the sandstone's textural and compositional characteristics and burial history. In this section we illustrate how Exemplar can be used to assess the effects of thermal history, timing of fluid overpressure development, grain size, and grain coating on reservoir quality. In addition, we show how the model can provide probabilistic predictions of reservoir quality prior to drilling when used in concert with Monte Carlo techniques.

Effect of Burial History on Porosity Loss

To illustrate the effects of burial history on model porosity predictions, we selected three quartzarenite sandstones that show a wide range in effective stress and temperature histories (Figure 5), but similar initial compositions and textures. The examples include (1) a Miocene sample from the Gulf of Mexico that was subject to rapid burial and early fluid overpressure development, (2) a Jurassic sample from the North Sea that developed fluid overpressures late in its burial history and has been exposed to high thermal gradients, and (3) a Cambrian sample from the Baltic region that experienced uplift and subsequent burial. Input for the simulations was derived from the petrographic data of Freeman (1990), Walderhaug (1994), and S. Bloch (1993, personal communication), and the burial histories of Shaw and Lander (1994), Walderhaug (1994), and Brangulis et al. (1993). Parameters for the compaction and quartz cementation models are identical for all three simulations.

Despite similar initial texture and composition, model results for the three sandstones indicate substantial differences in the relation of porosity to paleoburial depth, and show a much more complex porosity decline function than that ordinarily predicted by porosity models (Figure 6A). Model results show that essentially all porosity loss is due to compaction for samples at paleoburial depths of less than 1500 m, as shown by the IGV/depth

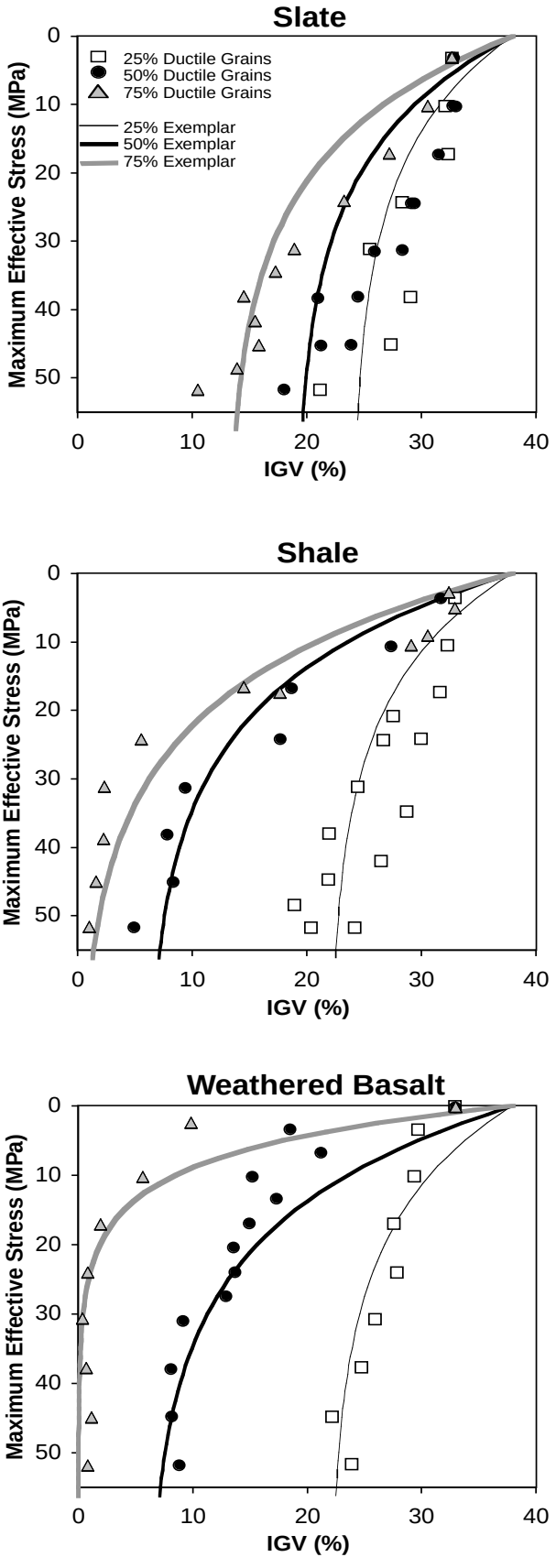

Figure 3—Calibration of the compaction model to sandstones with a variety of types and abundances of ductile grains. The experimental data, from Pittman and Larese (1991), are shown by the symbols, and the calibrated model results are shown by the lines. IGV = intergranular volume.

(Figure 6B) and bulk rock volume/depth plots (Figure 6C). The extent of shallow compaction is similar for the Baltic and North Sea examples because both are assumed to have been under hydrostatic fluid pressures over this interval. By contrast, the early and extensive fluid overpressures experienced by the Gulf of Mexico example significantly reduced the extent of compaction (Figure 6B). Although the North Sea example also presently occurs within a zone of extensive fluid overpressure, the development of the overpressure is assumed to have occurred after the sandstone had been buried to approximately 2500 m (Figure 5C). Simulations suggest that such deep overpressure development has little effect on porosity because compaction essentially is complete by this

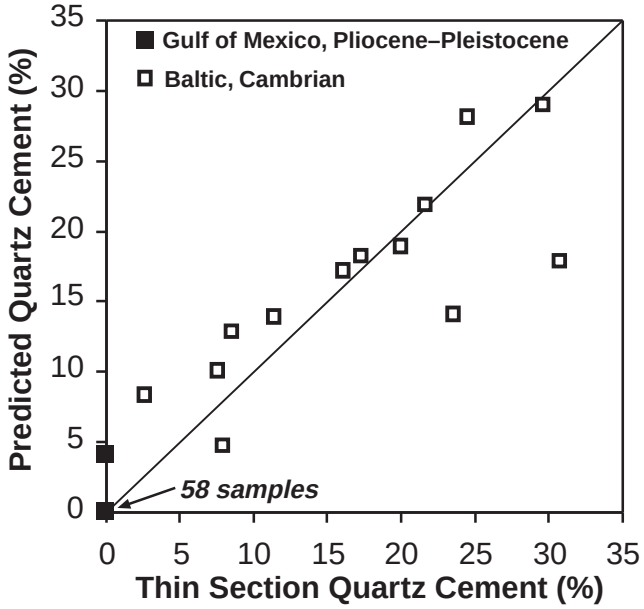

Figure 4—Comparison of predicted and measured quartz cement abundances for samples representing end members in heating rates using quartz cementation kinetics calibrated to Jurassic samples from the Norwegian continental shelf. The model provides accurate predictions for shallow Cambrian samples from the Baltic region [petrographic data from S. Bloch (1993, personal communication); burial history data from Brangulis et al. (1993)], as well as for deeply buried Pliocene–Pleistocene samples from the Gulf of Mexico Basin [petrographic data of Milliken (1985)].

depth and thus is irreversible. Note that although the high fluid overpressures experienced by the Gulf of Mexico example have reduced the extent of compaction, the sample experienced rates of compaction that are many times that of the North Sea and Baltic samples (Figure 6E). High rates of stress increase may explain the common occurrence of fractured grains in these rocks (Freeman, 1990).

Although the North Sea and Baltic examples show that elapsed time plays no role in simulated porosity loss due to compaction (except when effective stress varies), time is a critical control on the extent of quartz cementation when paleotemperatures exceed 70°C (approximately 1500 m burial). The effect of time is particularly well illustrated by the Baltic example by comparing predicted quartz cement fractions at 2200 m of burial (Figure 6D) as a function of the sandstone's burial history (Figure 5A). The modeled quartz cement fraction increases from 4% during the initial burial phase to 2200 m to 15% after the 260-m.y. period during which uplift and renewed subsidence returned the sample to 2200 m. By contrast, models that relate porosity to thermal indicators such as vitrinite reflectance would predict that porosity would remain essentially constant over this interval.

The model suggests that small, but significant, volumes of quartz cement can precipitate at comparatively shallow depths given sufficient time. This is shown by the Baltic sandstone, which is modeled to have about 2% quartz cement at a paleoburial depth of 1750 m. Small amounts of quartz cement at such shallow depths could act to significantly strengthen the rock framework, thereby retarding compaction. Such a scenario is consistent with the anomalously high IGV values displayed by the Baltic data set (34 ±6%) (S. Bloch, 1993, personal communication).

Temperature also plays a critical role in controlling quartz cementation, as is illustrated by the model behavior for North Sea and Baltic samples. Higher temperatures associated with the high thermal gradients and greater burial of the North Sea example resulted in net rates of quartz cementation that are over an order of magnitude greater than the greatest displayed by the Baltic sample (Figure 6F).

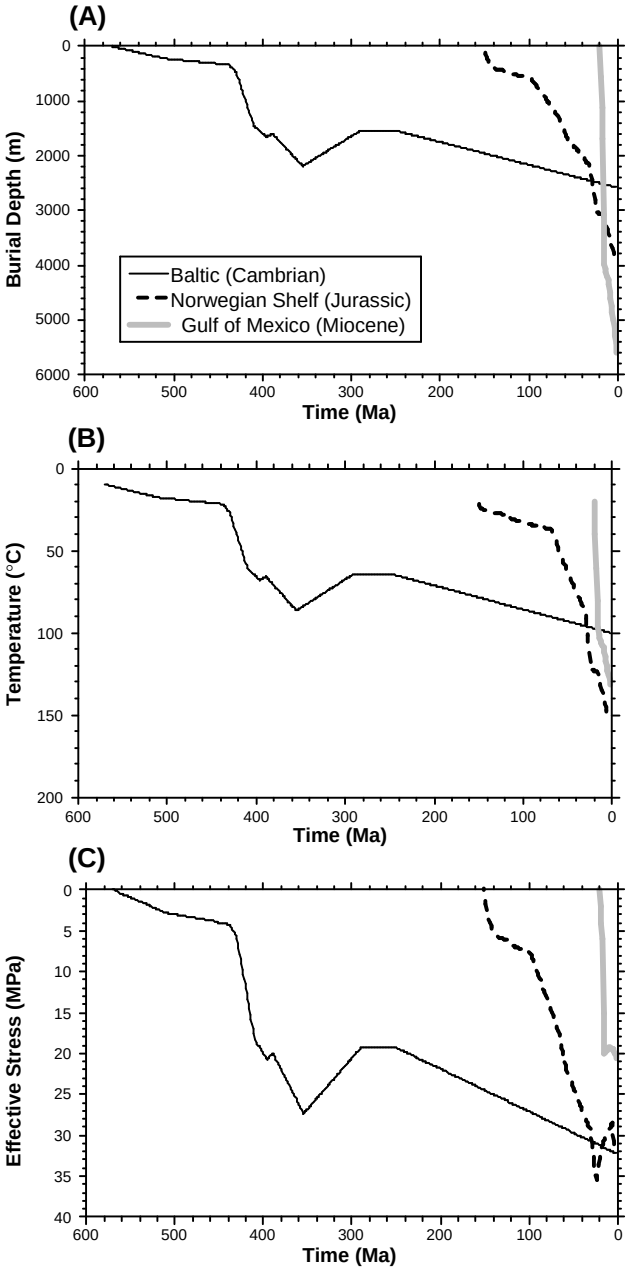

Figure 5—Burial history input data used for comparison in modeled compaction and quartz cementation as a function of burial history for the Baltic, the Norwegian shelf, and the Gulf of Mexico Basin. (A) Burial depth history. (B) Temperature history. (C) Effective stress history. The data used as input for the simulations were derived from the burial histories of Brangulis et al. (1993), Shaw and Lander (1994), and Walderhaug (1994).

Effect of Grain Coating on Porosity Loss

Grain coatings have long been recognized as a critical control on quartz cementation in sandstones because they can prevent or impede the nucleation of syntaxial quartz overgrowths on detrital quartz grains [see review by Ehrenberg (1993)]. Coatings commonly are made up of authigenic chlorite (Ehrenberg, 1993), microcrystalline quartz (Ramm and Forsberg, 1991; Ramm, 1994; Aase et al., 1996), siderite (R. E. Larese, 1997, personal communication), and detrital clay and Fe-oxyhydroxides.

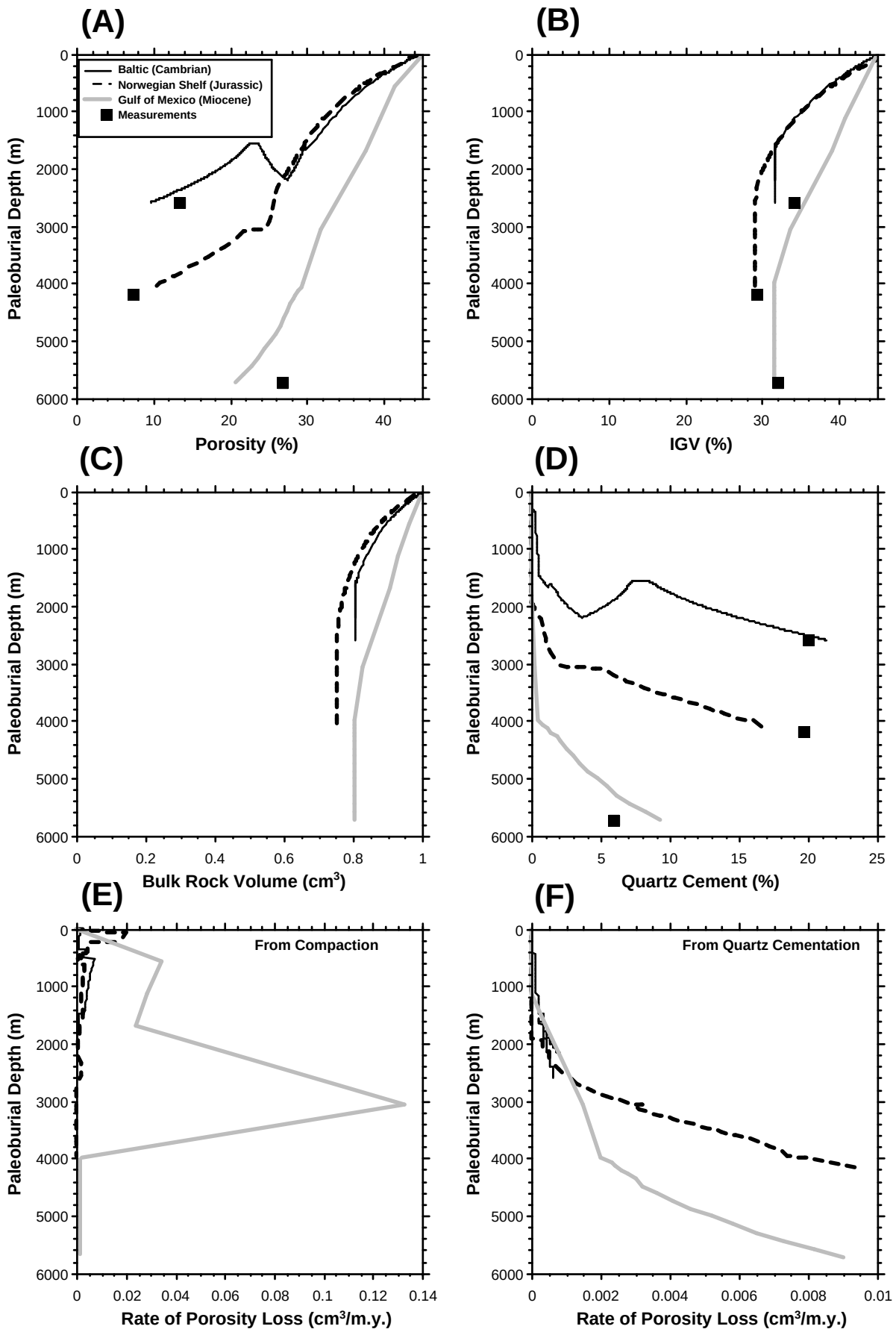
(A)
Baltic (Cambrian)
Norwegian Shelf (Jurassic)
Gulf of Mexico (Miocene)
Measurements
Paleoburial Depth (m)
Porosity (%)
(B)
IGV (%)
(C)
Bulk Rock Volume (cm3)
(D)
Quartz Cement (%)
(E)
From Compaction
Rate of Porosity Loss (cm3/m.y.)
(F)
From Quartz Cementation
Rate of Porosity Loss (cm3/m.y.)

Figure 6—Comparison of modeled compaction and quartz cementation as a function of burial history for samples with widely varying burial histories (shown in Figure 5), but similar initial textures and compositions. (A) Porosity with paleoburial depth. (B) IGV (intergranular volume) with paleoburial depth. (C) Bulk rock volume with paleoburial depth. (D) Quartz cement abundance with paleoburial depth. (E) Rate of porosity loss due to compaction with paleoburial depth. (F) Rate of porosity loss due to quartz cementation with paleoburial depth. Measured data are shown with the solid squares on (A), (B), and (D).

Perhaps the most conclusive study to date relating the textural effect of grain coating chlorite on quartz cementation is that of Byrnes and Wilson (1994) on the St. Peter and Mt. Simon sandstones of the Illinois basin. These workers showed that although there is no simple relationship between the overall abundance of chlorite with quartz cement, there is a systematic trend in quartz cement abundance with the visually estimated completeness of chlorite coating on quartz grains (Figure 7).

The relationship between grain coating and quartz cement abundance is well matched by Exemplar predictions based on the petrographic data of Byrnes and Wilson (1994) and the burial history reconstruction of Bethke et al. (1991) (Figure 7). Model predictions for the average composition and grain size come close to matching the median measured values. In addition, much of the variation in quartz cement abundance for a given grain coating can be accounted for by grain size variations, as illustrated by the model results for grain sizes one standard deviation toward coarser and finer textures as reported by Byrnes and Wilson (1994). An apparent discrepancy between the measurements and the model occurs at 100% grain coating, where the model predicts no quartz

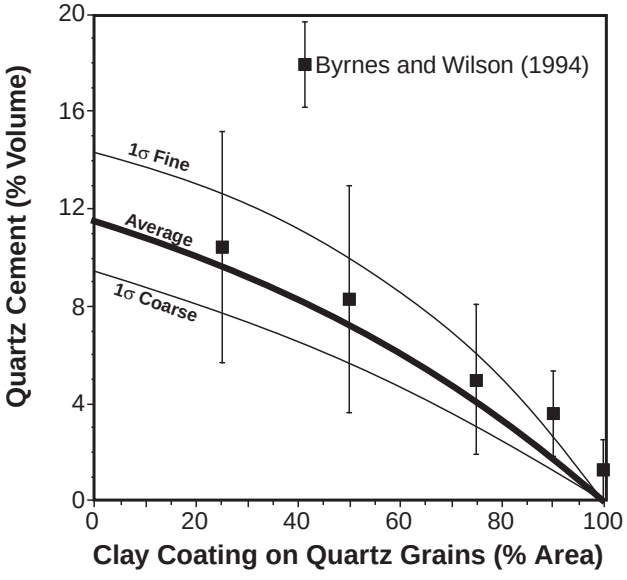

Figure 7—The completeness of grain coatings and quartz cement abundance for St. Peter and Mt. Simon sandstones from the Illinois basin. The measured data are from Byrnes and Wilson (1994), and the curves are model results using petrographic data of Byrnes and Wilson (1994) and burial history results of Bethke et al. (1991) as input.

Table 4. Input Uncertainties Used for Monte Carlo Example

	Distribution	Reservoir 1	Reservoir 2
Composition			
Initial porosity	Normal	45 ±3%	45 ±3%
Initial quartz grain	Normal	44 ±5%	36 ±5%
Initial matrix	Normal	1.5 ±2.0%	1.5 ±2.0%
Grain size	Normal	0.25 ±0.07 mm	0.21 ±0.05 mm
Grain coating	Normal	2 ±0%	2 ±0%
Burial History*			
Temperature 21 Ma	Triangular	80–115°C	100–150°C
Mbd 21 Ma	Triangular	1700–2570 m	2500–3800 m
Temperature 64 Ma	Triangular	75–110°C	105–140°C
Mbd 64 Ma	Triangular	1500–1925 m	2400–3000 m
Temperature 89 Ma	Normal	102 ±10°C	130 ±10°C
Mbd 89 Ma	Normal	1940 ±200 m	2910 ±200 m
Model Algorithms			
Quartz kinetics "b"	Normal	0.022 ±0.001 mol/cm²s	0.022 ±0.001 mol/cm²s
Minimum temperature for quartz cementation	Normal	70 ±7°C	70 ±7°C
β**	Log normal	0.06 ±0.01 MPa^{-1}	0.06 ±0.01 MPa^{-1}
IGV_f†	Normal	27 ±2%	22 ±3%

*Burial depth and temperature uncertainties are defined with correlation coefficients of 0.9. Mbd = maximum burial depth.
**β = exponential rate of intergranular volume loss with effective stress (1/MPa).
†IGV_f = stable packing intergranular volume.

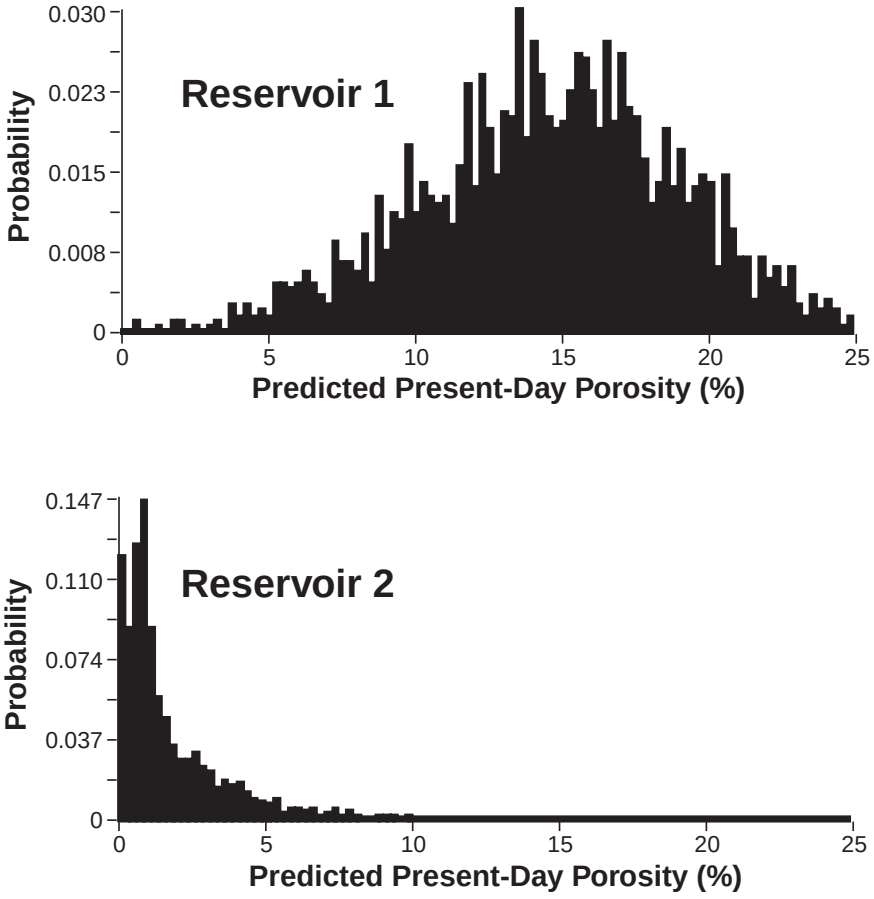

Figure 8—Probable distribution in porosity given uncertainties in model input parameters for two potential reservoir intervals in a prospect from a frontier setting. Each Monte Carlo simulation incorporates 2000 realizations.

cement, whereas measurements indicate as much as 2% cement (Figure 7). Model results consistent with the median value of 1.2% quartz cement suggest that, on average, approximately 3% of the quartz grain surfaces are uncoated. This value, in fact, is consistent with the 10% gap between the 90 and 100% categories used by Byrnes and Wilson (1994) in their visual estimations. Thus, the model appears to be robust given the uncertainties in the individual sample grain sizes, the measurement technique for grain coating, and the burial histories of the samples.

A Stochastic Approach to Reservoir Quality Prediction

Monte Carlo techniques provide a means of more rigorously assessing the probable porosity for a prospective reservoir by incorporating uncertainties and variabilities in model input data. In addition, when coupled with sensitivity analysis, Monte Carlo methods can be a useful aid in the quest to reduce predictive uncertainty because they help identify the input parameters that cause the greatest variability in the model predictions.

Uncertainties in the sandstone depositional texture and composition are best obtained through analysis of petrographic data and depositional models for mature basin areas, or analog settings for frontier regions. Uncertainties in burial history data are derived through basin modeling sensitivity studies. To obtain uncertainties in the input parameters for the compaction and quartz cementation algorithms, we use optimization techniques to find values that match thin section point-count analyses given the "most likely" burial history input. The collective distribution of values obtained through optimization of a suite of petrographically analyzed samples can then be used to define the uncertainties in the parameters used in the compaction and quartz cementation algorithms.

Once the input parameter uncertainties are defined, it is a relatively simple matter to conduct a Monte Carlo simulation. An arbitrary number of individual simulations are run (typically numbering in the thousands) to obtain a frequency distribution for the output parameter of interest. As an example, we have taken an undrilled prospect with two potential reservoir intervals. The most significant of the input uncertainties are summarized in Table 4.

Table 5. Sensitivity Results from Monte Carlo Example as Indicated by Contribution to Variance*

	Reservoir 1	Reservoir 2
Composition		
Inital quartz grain	4.5	10.8
Initial matrix	6.0	2.8
Grain size (mm)	17.9	33.0
Burial History		
Mbd** and °C, 21 Ma	22.0	10.6
Mbd and °C, 64 Ma	10.2	7.3
Mbd and °C, 89 Ma	14.9	4.7
Model Algorithms		
Quartz kinetics "b"	16.9	26.7
Minimum IGV†	6.7	3.7
Sum	99.1	99.6

*All units are in % of contribution to variance.
**Mbd = maximum burial depth.
†IGV = intergranular volume.

Uncertainties in the burial history were derived from basin modeling sensitivity studies, and uncertainties in the initial sandstone textures and compositions are based on analog data from nearby subbasins, together with regional depositional models. Uncertainties in model parameters are based on optimization studies in other regions. Simulations suggest probable porosity values of 14.9 ±4.4% and 3.1 ±2.6% for reservoirs 1 and 2, respectively (Figure 8). The simulations also show that whereas 85% of the reservoir 1 simulations have greater porosity than the economic cutoff of 10%, only 0.2% of the reservoir 2 simulations have greater porosity than the economic cutoff despite their occurrence at the same well location. We also ranked the input parameters with respect to their effect on the variability in the present-day porosity prediction by determining the contribution to variance (Table 5). The analysis indicates that whereas the greatest contribution to predicted variations in porosity for reservoir 1 is associated with uncertainties in the burial history, reservoir 2 is most sensitive to uncertainty in grain size and the kinetic parameters for quartz cementation.

CONCLUSIONS

Exemplar provides useful insights into the evolution of sandstone porosity through geologic time. The model accuracy is reasonably good in view of the uncertainties in both calibration and input data for the test data sets, and in that it reproduces measured IGV and quartz cement from samples exposed to a wide range of burial histories. Exemplar porosity predictions can be made in probabilistic terms through the application of parameter optimization and Monte Carlo techniques.

REFERENCES CITED

Aase, N. E., P. A. Bjørkum, and P. H. Nadeau, 1996, The effect of grain-coating microquartz on preservation of reservoir porosity: AAPG Bulletin, v. 80, p. 1654–1673.

Ajdukiewicz, J. M., S. T. Paxton, and J. O. Szabo, 1991, Deep porosity preservation in the Norphlet Formation, Mobile Bay, Alabama (abs.): AAPG Bulletin, v. 75, p. 533.

Athy, L. F., 1930, Density, porosity, and compaction of sedimentary rocks: AAPG Bulletin, v. 14, p. 1–24.

Atkins, J. E., and E. F. McBride, 1992, Porosity and packing of Holocene river, dune, and beach sands: AAPG Bulletin, v. 76, p. 339–355.

Awwiller, D. N., and L. L. Summa, 1997, Quartz cement volume constraints on burial history analysis: an example from the Eocene of western Venezuela (abs.): AAPG Annual Convention Program, p. A6.

Beard, D. C., and P. K. Weyl, 1973, Influence of texture on porosity and permeability of unconsolidated sand: AAPG Bulletin, v. 57, p. 349–369.

Bethke, C. M., J. D. Reed, and D. F. Oltz, 1991, Long-range petroleum migration in the Illinois basin: AAPG Bulletin, v. 75, p. 925–945.

Bjørkum, P. A., 1994, How important is pressure in causing dissolution of quartz? (abs.): AAPG Annual Convention Program and Abstracts, v. 3, p. 105.

Bloch, S., 1991, Empirical prediction of porosity and permeability in sandstones: AAPG Bulletin, v. 75, p. 1157–1160.

Bloch, S., 1994a, Importance of reservoir prediction in exploration, *in* M. D. Wilson, ed., Reservoir quality assessment and prediction in clastic rocks: SEPM Short Course 30, p. 5–8.

Bloch, S., 1994b, Secondary porosity in sandstones: significance, origin, relationship to subaerial unconformities, and effect on predrill reservoir quality prediction, *in* M. D. Wilson, ed., Reservoir quality assessment and prediction in clastic rocks: SEPM Short Course 30, p. 137–160.

Bloch, S., 1994c, Case history—offshore mid-Norway/Taranaki Basin, New Zealand/San Emigdio area, California, *in* M. D. Wilson, ed., Reservoir quality assessment and prediction in clastic rocks: SEPM Short Course 30, p. 357–366.

Bloch, S., and K. P. Helmold, 1994, Approaches to predicting reservoir quality in sandstones: AAPG Bulletin, v. 79, p. 97–115.

Brangulis, A. P., S. V. Kanev, L. S. Margulis, and R. A. Pomerantseva, 1993, *in* J. R. Parker, ed., Geology and hydrocarbon prospects of the Paleozoic of the Baltic region: Petroleum Geology of Northwest Europe, Proceedings of the 4th Conference: The Geological Society, London, p. 651–656.

Byrnes, A. P., and M. D. Wilson, 1994, Chapter 22. Case History—St. Peter and Mt. Simon Sandstones, Illinois Basin, *in* M. D. Wilson, ed., Reservoir quality assessment and prediction in clastic rocks: SEPM Short Course 30, p. 385–394.

Clarke, R. H., 1979, Reservoir properties of conglomerates and conglomeratic sandstones: AAPG Bulletin, v. 63, p. 799–809.

Dickinson, W. W., and J. D. Ward, 1994, Low depositional porosity in eolian sands and sandstones, Namib Desert: Journal of Sedimentary Research, v. A64, p. 226–232.

Dunn, T. L., 1994, Recognizing tectonic and compaction driven quartz grain fracturing and annealing in the Almond Formation, Green River basin, Wyoming (abs.): AAPG Annual Convention Program and Abstracts, v. 3, p. 140.

Ehrenberg, S. N., 1989, Assessing the relative importance of compaction processes and cementation to reduction of porosity evolution of Pliocene sandstones, Ventura basin, California: Discussion: AAPG Bulletin, v. 73, p. 1274–1276.

Ehrenberg, S. N., 1990, Relationship between diagenesis and reservoir quality in sandstones of the Garn Formation, Haltenbanken, mid-Norwegian continental shelf: AAPG Bulletin, v. 74, p. 1538–1558.

Ehrenberg, S. N., 1991, Kaolinized, potassium-leached zones at the contacts of the Garn Formation, Haltenbanken, mid-Norwegian continental shelf: Marine and Petroleum Geology, v. 8, p. 250–269.

Ehrenberg, S. N., 1993, Preservation of anomalously high porosity in deeply buried sandstone by grain-coating chlorite: examples from the mid-Norwegian continental shelf: AAPG Bulletin, v. 77, p. 1260–1286.

Freeman, C. W., 1990, Diagenesis of Miocene sandstones and shales, southern Louisiana Gulf Coast: Master's thesis, University of Missouri, Columbia, Missouri, 94 p.

Füchtbauer, H., 1967, Influences of different types of diagenesis on sandstone porosity: Proceedings of 7th World Petroleum Congress, v. 2, p. 353–369.

Giles, M. R., and R. B. de Boer, 1990, Origin and significance of redistributional secondary porosity: Marine and Petroleum Geology, v. 6, p. 261–269.

Heald, M. T., 1956, Cementation of Simpson and St. Peter sandstones in parts of Oklahoma, Arkansas, and Missouri: Journal of Geology, v. 58, p. 624–633.

Houseknecht, D. W., 1988, Intergranular pressure solution in four quartzose sandstones: Journal of Sedimentary Petrology, v. 58, p. 228–246.

Kurkjy, K. A., 1988, Experimental compaction studies of lithic sands: Master's thesis, University of Miami, Miami, Florida, 101 p.

Land, L. S., and S. P. Dutton, 1978, Cementation of a Pennsylvanian deltaic sandstone: isotopic data: Journal of Sedimentary Petrology, v. 48, p. 1167–1176.

Lander, R. H., V. Felt, L. Bonnell, and O. Walderhaug, 1997a, Utility of sandstone diagenetic modeling for basin history assessment (abs.): AAPG Annual Convention Program, p. A66.

Lander, R. H., O. Walderhaug, and L. Bonnell, 1997b, Application of sandstone diagenetic modeling to reservoir quality prediction and basin history assessment: Memorias del I Congreso Latinoamericano de Sedimentología, Venezolana de Geólogos Tomo I, p. 373–386.

Laubach, S. E., 1997, A method to detect natural fracture strike in sandstones: AAPG Bulletin, v. 81, p. 604–623.

Lundegard, P. D., 1991, Sandstone porosity loss—a "big picture" view of the importance of compaction: Journal of Sedimentary Petrology, v. 62, p. 250–260.

McBride, E. F., T. N. Diggs, and J. C. Wilson, 1990, Compaction of Wilcox and Carrizo sandstones (Paleocene–Eocene) to 4420 m, Texas Gulf Coast: Journal of Sedimentary Petrology, v. 61, p. 73–85.

Meshri, I. D., 1990, An overview of chemical models and their relationship to porosity prediction in the subsurface, *in* I. D. Meshri and P. J. Ortoleva, eds., Prediction of reservoir quality through chemical modeling: AAPG Memoir 49, p. 45–53.

Milliken, K. L., 1985, Petrology and burial diagenesis of Plio–Pleistocene sediments, northern Gulf of Mexico: Ph.D. dissertation, University of Texas, Austin, Texas, 112 p.

Palmer, S. N., and M. E. Barton, 1987, Porosity reduction, microfabric and resultant lithification in UK uncemented sands, *in* J. D. Marshall, ed., Diagenesis of sedimentary sequences: Geological Society Special Publication 36, p. 29–40.

Paxton, S. T., J. O. Szabo, C. S. Calvert, and J. M. Ajdukiewicz, 1990, Preservation of primary porosity in deeply buried sandstones: a new play concept from the Cretaceous Tuscaloosa Sandstone of Louisiana (abs.): AAPG Bulletin, v. 74, p. 737.

Pittman, E. D., 1979, Porosity, diagenesis and productive capability of sandstone reservoirs: SEPM Special Publication 26, p. 159–173.

Pittman, E. D., and R. E. Larese, 1991, Compaction of lithic sands: experimental results and applications: AAPG Bulletin, v. 75, p. 1279–1299.

Ramm, M., 1994, Porosity depth trends in Upper Jurassic reservoirs, Norwegian central graben: an example of porosity preservation at deep burial by grain-coating microquartz (abs): AAPG Annual Convention Program and Abstracts, p. 241.

Ramm, M., and A. W. Forsberg, 1991, Porosity vs. depth trends in Upper Jurassic sandstones from the Cod Terrace area, central North Sea, *in* M. Ramm, ed., Porosity depth trends in reservoir sandstones: Ph.D. thesis, University of Oslo, Oslo, Norway, 308 p.

Schneider, F., M. Bouteca, and G. Vasseur, 1994, Validity of the porosity/effective stress concept in sedimentary basin modeling: First Break, v. 12, p. 321–326.

Shaw, C. A., and R. H. Lander, 1994, Testing the sensitivity of hydrocarbon migration and overpressure development to rock, fault, and fluid properties at the field scale (abs.): AAPG Annual Convention Program and Abstracts, v. 3, p. 257.

Siever, R., and W. N. Stone, 1994, Quantitative petrologic constraints on basin paleohydrologic models (abs.): AAPG Annual Convention Program and Abstracts, p. 258–259.

Sippel, R. F., 1968, Sandstone petrology, evidence from cathodoluminescence petrography: Journal of Sedimentary Petrology, v. 38, p. 530–554.

Suchecki, R. K., and S. Bloch, 1988, Complex quartz overgrowths as revealed by microprobe cathodoluminescence (abs.): AAPG Bulletin, v. 72, p. 252.

Sweeney, J. J., and A. K. Burnham, 1990, Evaluation of a simple model of vitrinite reflectance based on chemical kinetics: AAPG Bulletin, v. 74, p. 1559–1570.

Szabo, J. O., and S. T. Paxton, 1991, Intergranular volume (IGV) decline curves for evaluating and predicting compaction and porosity loss in sandstones (abs.): AAPG Bulletin, v. 75, p. 678.

Taylor, J. M., 1950, Pore space reduction in sandstones: AAPG Bulletin, v. 34, p. 710–716.

Thomson, A., 1959, Pressure solution and porosity, *in* H. A. Ireland, ed., Silica in sediments: SEPM Special Publication 7, p. 92–111.

Ungerer, P., J. Burrus, B. Doligez, P. Y. Chenet, and F. Bessis, 1990, Basin evaluation by integrated two-dimensional modeling of heat transfer, fluid flow, hydrocarbon generation, and migration: AAPG Bulletin, v. 74, p. 309–335.

Walderhaug, O., 1994, Precipitation rates for quartz cement in sandstones determined by fluid-inclusion microthermometry and temperature-history modeling: Journal of Sedimentary Research, v. A64, p. 324–333.

Walderhaug, O., 1996, Kinetic modeling of quartz cementation and porosity loss in deeply buried sandstone reservoirs: AAPG Bulletin, v. 80, p. 731–745.

Walderhaug, O., R. H. Lander, P. A. Bjørkum, E. H. Oelkers, K. Bjørlykke, and P. H. Nadeau, in press, Modelling quartz cementation and porosity in reservoir sandstones—examples from the Norwegian continental shelf, *in* R. Worden, ed., Quartz cementation in oil field sandstones: International Association of Sedimentologists Special Publication.

Waples, D. W., and H. Kamata, 1993, Modelling porosity reduction as a series of chemical and physical processes, *in* A. G. Dóre et al., eds., Basin modelling: advances and applications: Norwegian Petroleum Society Special Publication 3, p. 303–320.

Wilson, J. C., and E. F. McBride, 1988, Compaction and porosity evolution of Pliocene sandstones, Ventura basin, California: AAPG Bulletin, v. 72, p. 664–681.

Wilson, M. D., 1984, Clastic diagenesis, in Geology for engineers, short course notes: The Petroleum Society of the Canadian Institute of Mining, Metallurgy and Petroleum, Calgary Section, 24 p.

Wilson, M. D., 1994, Introduction, *in* M. D. Wilson, ed., Reservoir quality assessment and prediction in clastic rocks: SEPM Short Course 30, p. 1–4.

Wilson, M. D., and P. T. Stanton, 1994, Diagenetic mechanisms of porosity and permeability reduction and enhancement, *in* M. D. Wilson, ed., Reservoir quality assessment and prediction

in clastic rocks: SEPM Short Course 30, p. 59–119.
Wood, J. R., 1994, Geochemical models, *in* M. D. Wilson, ed., Reservoir quality assessment and prediction in clastic rocks: SEPM Short Course 30, p. 23–41.
Wood, J. R., and A. P. Byrnes, 1994, Alternate and emerging methodologies in geochemical and empirical modeling, *in* M. D. Wilson, ed., Reservoir quality assessment and prediction in clastic rocks: SEPM Short Course 30, p. 395–400.

ABOUT THE AUTHORS

Rob Lander

Rob Lander is a senior staff geologist with Geologica in Stavanger, Norway, where he has been involved in the development and application of diagenetic and basin models since 1993, when he joined Geologica's parent company, Rogaland Research. He obtained a Ph.D. in 1991 from the University of Illinois, where he studied the fluid-flow and geochemical controls on the alteration of volcanogenic sediments. While at Exxon Production Research from 1990 to 1993, he worked on simulations of fluid overpressure development.

Olav Walderhaug

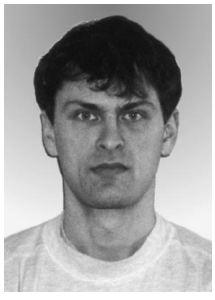

Olav Walderhaug is a staff geologist at Statoil's exploration technology division in Stavanger, Norway. He received his B.Sc. and M.Sc. degrees in petroleum geology from the University of Bergen, and a D.Sc. degree in sandstone diagenesis from the University of Oslo. His main research interests are within the field of sandstone diagenesis and related topics, including development of quantitative predictive models for quartz cementation and porosity evolution in reservoir sandstones.